Adaptive Control of a Flexible Manipulator With Unknown Hysteresis and Intermittent Actuator Faults

Shouyan Chen, Weitian He, Zhijia Zhao, *Member, IEEE*, Yun Feng, Zhijie Liu, *Member, IEEE*, and Keum-Shik Hong, *Fellow, IEEE*

***Abstract*—In this study, we consider a single-link flexible manipulator in the presence of an unknown Bouc-Wen type of hysteresis and intermittent actuator faults. First, an inverse hysteresis dynamics model is introduced, and then the control input is divided into an expected input and an error compensator. Second, a novel adaptive neural network-based control scheme is proposed to cancel the unknown input hysteresis. Subsequently, by modifying the adaptive laws and local control laws, a fault-tolerant control strategy is applied to address uncertain intermittent actuator faults in a flexible manipulator system. Through the direct Lyapunov theory, the proposed scheme allows the state errors to asymptotically converge to a specified interval. Finally, the effectiveness of the proposed scheme is verified through numerical simulations and experiments.**

***Index Terms*—Adaptive control, flexible manipulator, intermittent actuator faults, inverse hysteresis dynamics, vibration control.**

Manuscript received May 2, 2024; accepted June 26, 2024. This work was supported in part by the National Key Research and Development Program of China (2023YFB4706400), the National Natural Science Foundation of China (62273112, 62073030, 62203161), the Guangdong Basic and Applied Basic Research Foundation (2023B1515120018, 2023B1515120019), the Open Project of Xiangjiang Laboratory (23XJ03012), the Natural Science Foundation of Hunan Province (2024JJ5087), the Natural Science Foundation of Jiangxi Province (20232BAB212024), the National Research Foundation of Korea funded by the Ministry of Science and ICT, South Korea (IRIS-2023-00207954), the Science and Technology Planning Project of Guangzhou, China (2023A03J0120), and the Guangzhou University Research Project (RC2023037). Recommended by Associate Editor Zongyu Zuo. *(Corresponding author: Zhijia Zhao.)*

Citation: S. Chen, W. He, Z. Zhao, Y. Feng, Z. Liu, and K.-S. Hong, "Adaptive control of a flexible manipulator with unknown hysteresis and intermittent actuator faults," *IEEE/CAA J. Autom. Sinica*, vol. 12, no. 1, pp. 148–158, Jan. 2025.

S. Chen and Z. Zhao are with School of Mechanical and Electrical Engineering, Guangzhou University, Guangzhou 510006, China (e-mail: maxcsy@gzhu.edu.cn; zhaozj@gzhu.edu.cn).

W. He is with the School of Control Science and Engineering, Shandong University, Jinan 250061, China (e-mail: 202320743@mail.sdu.edu.cn).

Y. Feng is with the College of Electrical and Information Engineering, Hunan University, Changsha 410082, and also with the National Engineering Research Center for Robot Visual Perception and Control Technology, Hunan University, Changsha 410082, China (e-mail: fyrobot@hnu.edu.cn).

Z. Liu is with the School of Intelligence Science and Technology, University of Science and Technology Beijing (USTB), Beijing 100083, China (e-mail: liuzhijie@ustb.edu.cn).

K.-S. Hong is with the Institute for Future, the School of Automation, Qingdao University, Qingdao 266071, China, and also with the School of Mechanical Engineering, Pusan National University, Busan 46241, South Korea (e-mail: kshong@pusan.ac.kr).

Color versions of one or more of the figures in this paper are available online at http://ieeexplore.ieee.org.

Digital Object Identifier 10.1109/JAS.2024.124653

I. Introduction

In the wake of technological developments, modern industry has seen an increasing demand for lightweight and flexible materials, and flexible structures have garnered increasing attention [1]. As a typical flexible structure system, a flexible manipulator has the advantages of high flexibility, lightweight, and low energy consumption [2]. Flexible manipulators often generate vibrations and deformations under harsh environments and working conditions, which may cause adverse effects, such as deterioration of system performance and limited production accuracy. Therefore, an effective vibration control methodology to stabilize flexible manipulators needs to be established.

A flexible manipulator is an infinite-dimensional distributed-parameter system (DPS). If the system is simplified to a finite-dimensional state-space model for control design, adverse spillover effects may occur [3]. To overcome these problems, boundary control (BC) is considered to be a more effective control method for DPSs due to the simultaneous suppression of all modes of simplification of infinite-dimensional system dynamics. In recent years, significant progress has been achieved in BC of flexible manipulators. In [4], an adaptive event-triggered BC scheme was developed for a flexible manipulator with communication constraints. In [5], a boundary controller for a flexible manipulator was proposed based on a partial differential equation (PDE) robust observer. However, these studies were limited to vibration suppression, and the methods used did not apply to single-link flexible manipulator systems with input hysteresis.

Hysteresis is a dynamic nonlinearity that typically exists in electronic, electromagnetic, mechanical actuators, and other areas [6]–[9]. For systems with high control accuracy, hysteresis can cause phase shift and harmonic distortion problems related to the input signal information, resulting in an unstable control system. Several scholars have proposed various methods to solve this problem. In [10], an innovative event-based adaptive decentralized output feedback control scheme was introduced. A passive adaptive neural network control problem was addressed for multi-input multi-output nonstrict-feedback nonlinear systems subject to unmeasurable states and actuator hysteresis in [11]. In [12], a novel adaptive fault-tolerant control (FTC) was designed for a flexible Timoshenko arm to prevent actuator failures, backlash-like hysteresis, and external disturbances. In [13], an adaptive BC was

designed to suppress the vibrations of the flexible string, handle the uncertainties of the system parameters, and manage hysteresis nonlinearities. A novel adaptive control approach was introduced for the three-dimensional path-following of underactuated autonomous underwater vehicles, specifically designed to operate in environments affected by actuator hysteresis in [14]. In addition, the adaptive inverse compensation strategy is considered another effective method for handling hysteresis problems [15], [16]. In [17], perfect inverse dynamics were proposed for the Bouc-Wen hysteresis to compensate for hysteresis effects. The aforementioned approaches were conducted under the assumption that the hysteresis parameters were accurately known and were unavailable in the case of unknown hysteresis parameters. To eliminate this constraint, an adaptive hysteresis inverse output-feedback control scheme was developed in [18]. In [19], a novel indirect fuzzy control scheme with an alternative adaptive hysteresis inverse was proposed. However, the aforementioned unknown hysteresis inverse control was designed for systems represented by ordinary differential equations (ODEs) and cannot be applied to an infinite-dimensional flexible manipulator system with unknown hysteresis. To the best of our knowledge, although significant advancements in adaptive inverse control of ODE systems with unknown hysteresis have been achieved, limited studies have been conducted on addressing the simultaneous effects of unknown hysteresis and actuator faults in flexible manipulator systems; this motivates us to bridge the gap in research.

Owing to the complexity and multiple interferences of the working environment, actuator faults inevitably occur in various industrial controls [20]. In serious cases, sudden stucking or loss of partial effectiveness of an actuator may lead to an unstable system and even production accidents. FTC is considered an effective method for solving actuator faults. In recent years, research on FTC based on DPSs has progressed remarkably [21], [22]. In [23], an adaptive FTC scheme was developed to address actuator failures while suppressing the vibration of the system and achieving cooperative operation. The authors proposed an active adaptive FTC scheme for position tracking and vibration suppression of a constrained moving rigid-flexible manipulator system in [24]. The aforementioned FTC schemes consider a finite number of actuator faults, which cannot be directly used to handle infinite actuator faults. In an actual industrial process, actuator failure of a controlled system may occur more than once. To address this problem, a new adaptive failure/fault compensation control scheme was proposed for parametric strictly feedback nonlinear systems in [25]. In [26], a novel adaptive compensation strategy was proposed for a flexible manipulator in the presence of an infinite number of time-varying actuator faults. By contrast, the method in [26] was limited to eliminating the oscillation and compensating for infinite actuator faults, and intermittent actuator faults were not considered during the design. Although remarkable progress has been achieved in the FTC of flexible manipulators, no research has been conducted on adaptive inverse FTC to address the hybrid effects of unknown hysteresis nonlinearity and intermittent actuator faults in flexible manipulator systems.

Motivated by this background, we intend to develop a new adaptive compensation control for flexible manipulators with unknown hysteresis and intermittent actuator faults. The main contributions of this study are summarized as follows: 1) In contrast to previous studies [12], [13], [27], an adaptive inverse strategy is introduced and used to effectively counteract the input hysteresis effect in a flexible manipulator. In contrast to the control strategy in [17], this method can be applied to an unknown hysteresis problem. 2) A new neural network (NN)-based FTC is proposed to address intermittent actuator faults in a flexible manipulator system. In contrast to the literature [21], [22], the fault parameters in this study are time varying, and the faults occur frequently, rendering it more applicable to the actual situation. 3) The established control scheme can suppress the vibration of the controlled system without simplifying or discretizing the infinite-dimensional system dynamics, and the efficacy of the proposed controller is verified by numerical simulations and experiments.

Notations: The symbols in this article are standard. $\mathbb{Z}^+$ represents the set of all the positive integers. $\mathbb{R}$ represents all real numbers, with $\mathbb{R}^+ = \{x \in \mathbb{R} : x > 0\}$. $\mathbb{R}^{p\times q}$ denotes the set of all the real $p \times q$ matrices. $\|\boldsymbol{A}\|_F$ denotes the Frobenius norm of a matrix. $\boldsymbol{A} > 0$ represents a symmetric positive definite matrix. $\lambda_{\max}(\boldsymbol{A})$ represents the maximum eigenvalue of the symmetric matrix $\boldsymbol{A}$. For brevity, certain symbols are defined as $(\circ) = (\circ)(y,t)$, $(\dot\circ) = \partial(\circ)/\partial t$, $(\ddot\circ) = \partial^2(\circ)/\partial t^2$, $(\circ)' = \partial(\circ)/\partial y$, $(\circ)'' = \partial^2(\circ)/\partial y^2$, $(\circ)''' = \partial^3(\circ)/\partial y^3$, $(\circ)'''' = \partial^4(\circ)/\partial y^4$, $(\circ)_0 = \circ(0,t)$, $(\circ)_L = \circ(L,t)$, and $\tilde\circ = \circ - \hat\circ$.

II. Problem Statement

A. System Model

Fig. 1 depicts a schematic diagram of a flexible manipulator system, where YOZ and yOq represent the global inertial coordinate system and the local rotating reference frames with the joint, respectively. In addition, y is a spatial variable with $y \in [0, L]$ and t is the time variable with $t \in \mathbb{R}^+$. $z(y,t)$ represents the elastic deflection, and $\theta(t)$ represents the angular position of the joint. $\tau(t)$ denotes torque input and $q(y,t) = y\theta(t) + z(y,t)$ denotes the total displacement of the link in coordinate system YOZ.

First, we consider the dynamical model of the system as follows:

$$\rho\ddot q(y,t) + c\dot q(y,t) = -EIz''''(y,t) + Tz''(y,t) \tag{1}$$

$$EIz'''(L,t) = Tz'(L,t) \tag{2}$$

$$z(0,t) = z'(0,t) = z''(L,t) = 0 \tag{3}$$

$$I\ddot\theta(t) = EIz''(0,t) + Tz(L,t) + \tau(t) \tag{4}$$

where I, EI, ρ, T, and c denote the inertia of the joint, bending stiffness, linear density, tension, and the coefficient of viscosity, respectively.

B. Hysteresis Characteristic Analysis

In this study, we consider that the actuator input of the system is affected by the Bouc-Wen type of hysteresis, which is

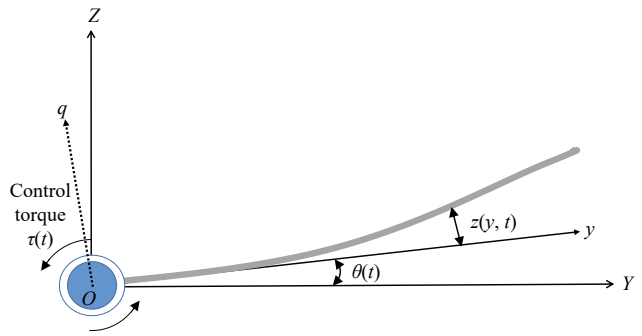

Fig. 1. Schematic of the considered flexible manipulator.

one of the most acceptable models for describing rate-dependent hysteresis [17], [28], [29], and it is represented as

$$u_f(t) = H(v(t)) = o\kappa v + (1-o)\kappa\zeta = \mu_1 v + \mu_2\zeta \tag{5}$$

where $0 < o < 1$ denotes the stiffness ratio and κ is a parameter related to the pseudo natural frequency. The constants μ_1 and μ_2 are unknown but share the same sign, with $\mu_1 = o\kappa$ and $\mu_2 = (1-o)\kappa$. $v(t)$ denotes the actual actuator inputs after inverse compensation. $u_f(t)$ represents the output of the input $v(t)$ after being affected by hysteresis. $\zeta \in \mathbb{R}$ is a rate-dependent variable that depends on input v with its derivative $\dot{v}$, expressed as

$$\dot{\zeta} = \dot{v} - \beta|\dot{v}||\zeta|^{n-1}\zeta - \chi\dot{v}|\zeta|^n = \dot{v}f(\zeta,\dot{v}) \tag{6}$$

where $\beta > |\chi|$ and $n \geq 1$. β and χ are parameters describing the shape and amplitude of the hysteresis. n governs the smoothness of the transition from the initial slope to the slope of the asymptote. $f(\zeta,\dot{v})$ is a function with two inputs ζ and $\dot{v}$ defined as

$$f(\zeta,\dot{v}) = 1 - \mathrm{sgn}(\dot{v})\beta|\zeta|^{n-1}\zeta - \chi|\zeta|^n. \tag{7}$$

Remark 1: In [27], [30], the authors proposed a BC method for DPSs with hysteresis. The proposed hysteresis model is a special case of the hysteresis model (5).

For convenience of the control design, we parameterize the hysteresis model (5) as

$$u_f(t) = \mu^T\aleph \tag{8}$$

where $\mu = [\mu_1,\mu_2]^T$ and $\aleph = [v,\zeta]^T$.

To address hysteresis parameter uncertainty, we introduce the following inverse dynamics [19]:

$$v(t) = \widehat{HI}(u_{fd}) = \frac{1}{\hat{\mu}_1}u_{fd} - \frac{\hat{\mu}_2}{\hat{\mu}_1}\zeta_d \tag{9}$$

$$\dot{\zeta}_d = \dot{u}_{fd}h_d(u_{fd},\zeta_d), \quad \zeta_d(0) = 0 \tag{10}$$

where u_{fd} is the control signal to be designed, and we define the function $h_d(u_{fd},\zeta_d)$ as

$$h_d(\dot{u}_{fd},\zeta_d) = 1 - \sigma_1\mathrm{sign}(\dot{u}_{fd})|\zeta_d|^{\epsilon-1}\zeta_d - \sigma_2|\zeta_d|^{\epsilon} \tag{11}$$

where σ_1, σ_2, and ϵ are design parameters. Invoking (9), the expressions of u_{fd} is given as

$$u_{fd}(t) = \hat{\mu}^T\aleph_d \tag{12}$$

where $\hat{\mu} = [\hat{\mu}_1,\hat{\mu}_2]^T$ denotes the estimates of $\mu = [\mu_1,\mu_2]^T$, and $\aleph_d = [v,\zeta_d]^T$.

Additionally, the compensation error can be expressed as

$$u_f - u_{fd} = \mu^T\aleph - \hat{\mu}^T\aleph_d = \tilde{\mu}^T\aleph_d + d(t) \tag{13}$$

where $d(t) = \mu_2(\zeta - \zeta_d)$, $\tilde{\mu}$ is the estimated error of μ defined as $\tilde{\mu} = \mu - \hat{\mu}$.

Remark 2: In contrast to previous studies [16], [17], [31], the inverse function can be designed directly without the use of parameter identification or knowledge of the specific hysteresis parameters. We assume that a positive constant D exists to ensure that the compensating error $d(t)$ satisfies the condition $d(t) \leq D = \sqrt[n]{1/(\beta+\chi)} + \sqrt[\epsilon]{1/(\sigma_1+\sigma_2)}$.

C. Intermittent Actuator Fault Model

According to [32], the intermittent actuator fault model is described as

$$\tau(t) = \sigma(t)u_f(t) + u_{f,h}(t), \quad \sigma(t) = \sigma_h, \quad h \in \mathbb{Z}^+ \tag{14}$$

where h indicates the number of faults, $t \in [t_{h,s}, t_{h,e})$, σ_h is an unknown efficiency factor satisfying $0 < \underline{\sigma} \leq \sigma_h \leq 1$. Note that $u_{f,h}(t) \leq \bar{u}_f$, and $\underline{\sigma}$, u_f are unknown constants. (14) indicates that the actuator loses $(1-\sigma_h)\times 100\%$ of its effectiveness and produces the floating bias fault $u_{f,h}(t)$ from time $t_{h,s}$ till $t_{h,e}$. When $\sigma(t) = \sigma_h$, the system becomes a common fault model that considers both the efficiency partial loss fault and the floating bias fault [21], [33]. This model did not take into account the reoccurrence of fault.

Remark 3: In common fault models (see (1) in [23]), the parameter σ representing the degree of actuator fault is typically an unknown but fixed constant, which does not vary over time. In contrast, in (14), σ is set as an unknown and time-varying parameter. This design is inspired by the real-world observation that some actuator faults may exhibit intermittent characteristics. This means that an actuator may repeatedly and automatically switch from a faulty state to a normal operating state or to other different fault states. As expressed in (14), an actuator with a fault might experience multiple failures. Therefore, the actuator fault model proposed in our study is more reflective of real industrial environments, making the corresponding control design more complex and challenging.

Thus, combined with (13), the actual inputs $\tau(t)$ can be expressed as

$$\tau(t) = \sigma(t)u_{fd}(t) + \sigma(t)\tilde{\mu}^T\aleph_d + \sigma(t)d(t) + u_{f,h}(t). \tag{15}$$

Remark 4: Differently from [12] and [22], intermittent faults in the actuator is assumed to occur in this paper, which is more common than the common fault model with only one single fault in the FTC results. It is worth noting that the fault-free condition is a special case of (14) when $\sigma(t) = 1$ and $u_{f,h}(t) = 0$.

Remark 5: In this study, we consider a single-link flexible manipulator encountering both unknown Bouc-Wen type hysteresis and intermittent actuator faults, which are plausible concurrent issues in real-world environments. A quintessential example is the robotic arm systems used in the aerospace domain. In the space environment, due to extreme tempera-

ture variations and microgravity conditions, the actuators of these arms are likely to experience hysteresis. This hysteresis, typically resulting from internal mechanical friction or material thermal expansion, causes input hysteresis. Concurrently, in such environments, the actuators might also suffer intermittent faults. These faults could stem from radiation damage to electronic components, impacts from tiny meteorite fragments, or prolonged wear and tear. In such instances, actuators might exhibit partial efficiency loss faults and floating bias faults without warning, only to return to normal operation after some time. Both phenomena could coexist in aerospace robotic arm systems, posing dual challenges to their performance and reliability. Therefore, the design and control strategies for such systems need to comprehensively address both phenomena to ensure that the robotic arms operate stably and efficiently in these complex conditions.

D. Radial Basis Function NN (RBFNN)

Because of its fixed and simple three-layer architecture, RBFNN is simpler in designing and training than other NNs [34]. In recent years, it has been widely used in the nonlinear control [35]. In this paper, the RBFNN is utilized to tackle coupling terms $\sigma(t)\aleph_d$ such that

$$\sigma(t)\aleph_d = p^{*T}H(W) + \varepsilon(W), \quad \|\varepsilon(W)\| \le \bar{\varepsilon} \tag{16}$$

where $W = [v, \zeta_d]^T$ and p^* stand for the input and ideal weight vectors, respectively. $\varepsilon(W)$ denotes the approximation error and $\bar{\varepsilon}$ is an unknown constant. $q \in \mathbb{Z}^+$ denotes the node number in the hidden layer. $H(W) = [H_1(W), H_2(W), \ldots, H_N(W)] \subset \mathbb{R}^N$ represents the Gaussian function as

$$H_i(W) = \exp\left[\frac{-(W-c_i)^T(W-c_i)}{b_i^2}\right], \ i = 1, 2, \ldots, N \tag{17}$$

where c_i is the center vector of the ith hidden layer neuron and $b_i \in \mathbb{R}^+$ is the width of the Gaussian function. Moreover, let $\hat{p}$ be the estimation of p^*, where $\|\tilde{p}\| = \|p^* - \hat{p}\|$.

E. Control Objective and Related Lemmas

This paper aims at presenting an adaptive inverse compensation control strategy for a flexible manipulator with intermittent actuator faults and unknown input hysteresis.

To facilitate the subsequent analysis, the following assumptions and lemmas are provided.

Lemma 1 [36]: Consider the first-order differential equations as follows:

$$\dot{s}(t) = \gamma_s f_s - \gamma_s \kappa_s (s(t) - s(0)) \tag{18}$$

where γ_s and κ_s are positive constants. If f_s, $s(0) \ge 0$, the solution of (18) is rendered to be non-negative for all $t \ge 0$.

Lemma 2 [19]: For any piecewise continuous signals v and $\dot{v}$, the output $\zeta(t)$ is bounded and satisfies $|\zeta(t)| < \sqrt[n]{1/(\beta+\chi)}$. Similarly, we get $|\zeta_d(t)| < \sqrt[6]{1/(\sigma_1+\sigma_2)}$.

Lemma 3 [37]: If e and r are scalars and satisfy $e \in \mathbb{R}$, $r \in \mathbb{R}^+$, we have

$$0 \le |e| - \frac{e^2}{\sqrt{e^2 + r^2}} < \bar{r}. \tag{19}$$

If r is a positive uniformly bounded continuous function with $r(t)$ satisfying $\lim_{t\to\infty} \int_{t_0}^{t} r(t)dt \le \bar{r} < \infty$, the above inequality is still satisfied, where $\bar{r}$ is a positive constant.

III. Control Design

In this section, an adaptive FTC is proposed to achieve control objectives. By combining the unknown compensation error with the time-varying actuator faults, an upper-bound adaptive law is proposed. Subsequently, the stability analysis is provided.

A. Adaptive FTC

We construct the auxiliary signal $u_a(t) = \alpha\dot{\theta}(t) + \beta_2[\theta(t) - \theta_d] = \alpha\dot{\theta}(t) + \beta_2\theta_e(t)$, and θ_d denotes the reference signal. Then, the control signal $u_{fd}(t)$ is designed as

$$u_{fd}(t) = -\hat{\varrho}\beta_1(t) \tag{20}$$

where $\beta_1(t) = -z_1(t)u_a(t)$. Let $\varrho = 1/\underline{\sigma}$ and $\hat{\varrho}$ represent the estimate value of ϱ. z_1 is given as

$$z_1(t) = k + \frac{1}{4\delta}\left[T z_L^2 + (k_1 + I\beta_2)\dot{\theta}^2(t) + k_\theta \theta_e^2(t) + \frac{\hat{\hbar}^2}{\sqrt{u_a^2(t)\hat{\hbar}^2 + r^2(t)}}\right] \tag{21}$$

where k, k_θ, and β_2 are positive constants, $\delta \ge 0.25$, and $k_1 \in \mathbb{R}$. $\hat{\hbar}$ is the estimation of the upper bound $\hbar$ defined as $\hbar = \|p_M\mu^T\| + \mu_M\bar{\varepsilon} + D + \bar{u}_f$. The definitions of p_M and μ_M can be found in Remark 6. Then, the parameter updating laws are designed as

$$\dot{\hat{\varrho}} = \gamma_\varrho z_1(t)u_a^2(t) - \gamma_\varrho\hat{\varrho} \tag{22}$$

$$\dot{\hat{\hbar}} = \gamma_h u_a(t) - \gamma_h\hat{\hbar} \tag{23}$$

$$\dot{\hat{\mu}} = \mathrm{Proj}_\mu\{\Gamma_\mu u_a(t)\hat{p}^T H(W)\} \tag{24}$$

$$\dot{\hat{p}} = -\mathrm{Proj}_p\{\Gamma_p(u_a(t)H(W)\hat{\mu}^T\} \tag{25}$$

where $\Gamma_\mu, \Gamma_p > 0$, with γ_ϱ and γ_h being positive constants.

To avoid singularity, making the control inputs infinite, the projection mapping Proj{∘} is used to limit the range of adaptive parameters $\hat{\mu}$ and $\hat{p}$, defined as [38]

$$\mathrm{Proj}_{\hat{\xi}}(\diamond) = \begin{cases} \left(\diamond - \Psi\dfrac{\nabla_{\hat{\xi}}\mathcal{P}\nabla_{\hat{\xi}}\mathcal{P}^T}{\nabla_{\hat{\xi}}\mathcal{P}^T\Psi\nabla_{\hat{\xi}}\mathcal{P}}\right)\diamond \\ \quad \text{if } \hat{\xi} \in \bar{\Omega} \text{ and } \nabla_{\hat{\xi}}\mathcal{P}^T\diamond > 0 \\ (\diamond), \ \text{if } \hat{\xi} \in \breve{\Omega} \\ \quad \text{or } \nabla_{\hat{\xi}}\mathcal{P}^T\diamond \le 0 \end{cases} \tag{26}$$

where $\Psi > 0$, $\nabla_{\hat{\xi}}\mathcal{P}$ denotes an outward normal vector at $\bar{\Omega}$, $\breve{\Omega}$ and $\bar{\Omega}$ denote the interior and the boundary of the set $\Omega \in \mathbb{R}$, respectively.

Remark 6: In this research, we utilize the adaptive mapping operator (26) to design the adaptive laws (24) and (25) for unknown parameters μ and p. Based on the mapping operator (26), the estimates of the unknown parameters $\hat{\mu}$ and $\hat{p}$ can

not exceed the established boundaries. Since the estimates are bounded and not divergent, the estimation errors $\|\tilde{\mu}\|$ and $\|\tilde{p}\|$ are also bounded. The proof process is similar to that of [26]. Here, we define the unknown constants μ_M and p_M such that $\|\tilde{\mu}\| \le \mu_M$ and $\|\tilde{p}\| \le p_M$.

Remark 7: It should be emphasized that the FTC strategy proposed in [21], [22] and [39]–[41] cannot directly be applied to this system. If the actuator experiences multiple faults, the parameter $\dot{\sigma}(t)$ will be unbounded, which may lead to system instability. To avoid the unbounded term $\frac{\sigma}{\gamma_\varrho}\tilde{\varrho}(\dot{\varrho}-\dot{\hat{\varrho}})$ appearing in the time derivative of subsequent Lyapunov functions $\dot{V}(t)$, we propose a novel FTC strategy, which is different from that in literature [26]. By introducing quadratic nonlinear damping terms β_1 and z_1, we can handle this issue effectively.

B. Stability Analysis

Consider the Lyapunov function candidate as

$$V(t) = V_1(t) + V_2(t) + V_3(t) \tag{27}$$

with

$$V_1(t) = \frac{\alpha}{2}\rho\int_0^L \dot{q}^2 dy + \frac{\alpha}{2}EI\int_0^L z''^2 dy + \frac{\alpha}{2}T\int_0^L z'^2 dy \tag{28}$$

$$V_2(t) = \frac{1}{2}Iu_a^2 + \frac{1}{2}k_\theta\theta_e^2 + \frac{1}{2}\tilde{\mu}^T\Gamma_\mu^{-1}\tilde{\mu} + \frac{\sigma}{2\gamma_\varrho}\tilde{\varrho}^2 + \frac{1}{2\gamma_h}\tilde{\hbar}^2 + \frac{1}{2}Tr\{\tilde{p}^T\Gamma_p^{-1}\tilde{p}\} \tag{29}$$

$$V_3(t) = \beta_2\rho\int_0^L \dot{q}(y,t)q_e(y,t)dy \tag{30}$$

where $q_e(y,t) = z(y,t) + y\theta_e(t)$. Obviously, $\dot{q}_e(y,t) = \dot{q}(y,t)$.

Lemma 4: The selected Lyapunnov function (27) satisfies the following property:

$$0 \le \lambda_2[V_1(t)+V_2(t)] \le V(t) \le \lambda_3[V_1(t)+V_2(t)] \tag{31}$$

where $\lambda_2 = 1-\lambda_1$ and $\lambda_3 = 1+\lambda_1$ are two positive constants with $\lambda_1 = \max\{\frac{\beta_2(1+L)}{\pi_1\alpha}, \frac{\beta_2\rho L^2\pi_1}{k_\theta\alpha}, \frac{\beta_2\rho L^2\pi_1}{T\alpha}\}$.

Proof: See Appendix A. ■

Lemma 5: The time derivative of the Lyapunov function (27) is proved to be bounded as

$$\dot{V}(t) \le -\lambda V(t) + \iota \tag{32}$$

where $\lambda, \iota \in \mathbb{R}^+$.

Proof: See Appendix B. ■

Theorem 1: For the flexible manipulator system described by (1)−(4) in the presence of unknown hysteresis and intermittent actuator faults, under the proposed control (20) and (21) and the parameter updating laws (22)−(25), we can deduce the following:

1) The elastic displacement $z(y,t)$ is uniformly bounded, starts in a compact set Ω_1, and converges eventually to another compact set Ω_2.

$$\Omega_1 = \{z(y,t) \in \mathbb{R} \,|\, |\, z(y,t) \,| \le \Phi_1\}$$
$$\Omega_2 = \{z(y,t) \in \mathbb{R} \,|\, \lim_{t\to\infty} |\, z(y,t) \,| \le \Phi_2\} \tag{33}$$

where $\Phi_1 = \sqrt{\frac{2L}{\alpha T\lambda_1}[V(0)+\frac{\iota}{\lambda}]}$ and $\Phi_2 = \sqrt{\frac{2\iota}{\alpha T\lambda_1\lambda}}$.

2) The angular error $\theta_e(t)$ is maintained in the compact set Ω_3 and finally converges to the compact set Ω_4.

$$\Omega_3 = \{\theta_e(t) \in \mathbb{R} \,|\, |\, \theta_e(t) \,| \le \Phi_3\}$$
$$\Omega_4 = \{\theta_e(t) \in \mathbb{R} \,|\, \lim_{t\to\infty} |\, \theta_e(t) \,| \le \Phi_4\} \tag{34}$$

where $\Phi_3 = \sqrt{\frac{2L}{k_\theta\lambda_1}[V(0)+\frac{\iota}{\lambda}]}$ and $\Phi_4 = \sqrt{\frac{2L\iota}{k_\theta\lambda_1\lambda}}$.

Proof: Multiplying (32) by $e^{\lambda t}$ yields

$$\frac{\partial}{\partial t}[V(t)e^{\lambda t}] \le \iota^{\lambda t}. \tag{35}$$

Substituting (35), we obtain

$$V(t) \le [V(0) - \frac{\iota}{\lambda}]e^{-\lambda t} + \frac{\iota}{\lambda}. \tag{36}$$

Using (28) and the Sobolev's inequality (see Lemma 2 in [42]) yields

$$\frac{1}{2L}\alpha T z^2(y,t) \le \frac{\alpha}{2}T\int_0^L z'^2(y,t)dy \le V_1(t) \le \frac{1}{\lambda_1}V(t). \tag{37}$$

Invoking (37), (36) is rewritten as

$$|z(y,t)| \le \Phi_1 = \sqrt{\frac{2L}{\alpha T\lambda_1}[V(0)+\frac{\iota}{\lambda}]}. \tag{38}$$

Further, we have

$$\lim_{t\to\infty}|z(y,t)| \le \Phi_2 = \sqrt{\frac{2\iota}{\alpha T\lambda_1\lambda}}, \ \forall y \in [0,L]. \tag{39}$$

Similarly, from (29), we have

$$|\theta_e(t)| \le \Phi_3 = \sqrt{\frac{2L}{k_\theta\lambda_1}[V(0)+\frac{\iota}{\lambda}]}, \ \forall t \in [0,+\infty). \tag{40}$$

Then, we arrive at

$$\lim_{t\to\infty}|\theta_e(t)| \le \Phi_4 = \sqrt{\frac{2L\iota}{k_\theta\lambda_1\lambda}}, \ \forall t \in [0,+\infty). \tag{41}$$

■

Remark 8: The control parameters are selected to satisfy Lemma 4 and constraint conditions (58)–(62) at the same time. The process of selecting parameters is described as follows. First, we choose appropriate parameters π_1 and β_2 to complete the proof of Lemma 4. Next, choosing appropriate parameters k, k_θ, k_1, π_1, π_2, and π_3, the ϖ_i, $i = 1,\ldots,4$ and ι are satisfied. Thus, the proof of Lemma 5 is completed. Through Lemma 5, we can then derive (39) and (41), which define the convergence interval for the error.

IV. Numerical Simulation

To verify the effectiveness of the proposed control strategy, the finite difference method is used for the numerical simulation. The system parameters selected are $EI = 0.157\ \text{Nm}^2$, $T = 0.1\ \text{N}$, $L = 0.419\ \text{m}$, $\rho = 0.1\ \text{kg/m}$, $c = 0.04\ \text{NS/m}$, and $I = 0.0038\ \text{kgm}^2$. In this study, the simulation time and space steps are set as $\triangle t = 3.75\times10^{-5}\ \text{s}$ and $\triangle y = 0.0221\ \text{m}$, respec-

tively. The desired trajectory θ_d is selected as $\frac{\pi}{12}$. The initial states of the system are $z(y,0) = 0.5\,\mathrm{s}^2\,\mathrm{m}$, $\dot{z}(y,0) = 0\,\mathrm{m/s}$, $\theta(0) = 0\,\mathrm{rad}$, and $\dot{\theta}(0) = 0\,\mathrm{rad/s}$. We consider a flexible manipulator with intermittent actuator faults.

$$\tau(t) = \begin{cases} 0.5u_f(t) + 0.1e^{-0.2t}, & \text{if } t \in [g-1, g) \\ u_f(t), & \text{otherwise} \end{cases} \tag{42}$$

where g is an odd positive number.

The parameters selected for the hysteresis inverse fault-tolerant controller (HIFTC) are $\alpha = 1$, $\beta_2 = 0.05$, $\delta = 0.8$, $k_\theta = 4.5$, $r(t) = 0.7 + 0.5e^{-0.2t}$, $k = 1$, and $k_1 = 0.2$. The parameter-updating laws are selected as $\gamma_\varrho = 0.1$, $\gamma_h = 0.1$, $\hat{\mu}(0) = [0.32, 0.32]^T$, $\hat{h}(0) = 0.3$, $\hat{p}(0) = 0$, and $\hat{\varrho}(0) = 1$. This set is given by $\Omega = \{\hat{\mu} \in \mathbb{R}^2 | 0.2 \le \hat{\mu}_1 < 0.4, 0.2 \le \hat{\mu}_2 < 0.4\}$. The hysteresis parameters are $\mu_1 = 0.3$, $\mu_2 = 0.3$, $\beta = 1$, $n = 1.2$, and $\chi = 0.8$. Fig. 2 shows that the deflection $z(y,t)$ of the entire flexible link under the HIFTC approaches to zero within 1.5 s.

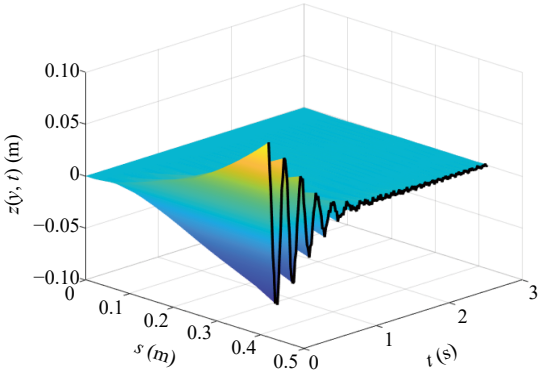

Fig. 2. Deflection of the flexible link under the HIFTC controller.

To further verify the effectiveness of the proposed control, we also provide simulation results with the following proportional differentiation controller (PDC) in [26] and BC in [43].

The PDC in [26] is expressed as

$$\tau(t) = -k_d\dot{\theta}(t) - k_p\theta_e(t) \tag{43}$$

where $k_d = 2$ and $k_p = 8$.

The BC in [43] is given as

$$\tau(t) = -ku_a(t) - (k_1 + T)z_L - I\beta_2\dot{\theta}(t) - k_\theta\theta_e(t) \tag{44}$$

where $k = 0.09$, $k_1 = 0.1$, $\beta_2 = 0.05$, and $k_\theta = 5$.

We can observe from Figs. 3 and 4 that the HIFTC can maintain excellent control performance under the influence of input hysteresis and intermittent actuator faults. Compared with BC and PDC, the proposed controller can quickly track the reference signal θ_d while maintaining the system stability. In addition, the end-point offset $z(L,t)$ of the flexible manipulator can also approach to zero within 1.5 s under the HIFTC. Although the offset $z(L,t)$ is convergent under BC and PDC, after 1.5 s, the angle $\theta(t)$ still does not converge to the reference signal θ_d and some steady-state error occurs. Fig. 5 depicts the control inputs. By applying hysteresis inverse dynamics (9), the actual input u_f of the system fits the expected input u_{fd}. Simultaneously, when the actuator loses 50% of its effectiveness, the stability of the control system is

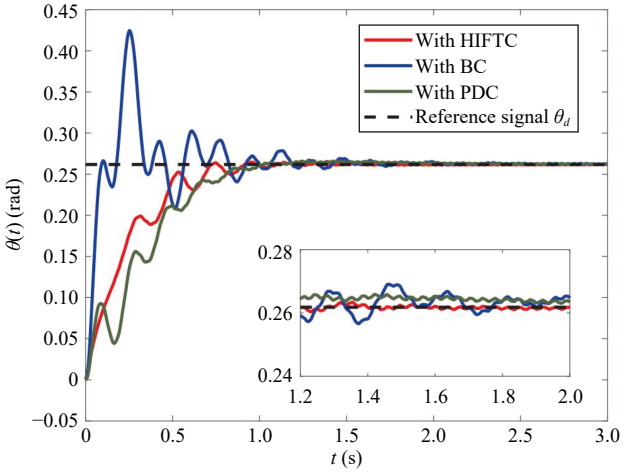

Fig. 3. Tracking of angle $\theta(t)$.

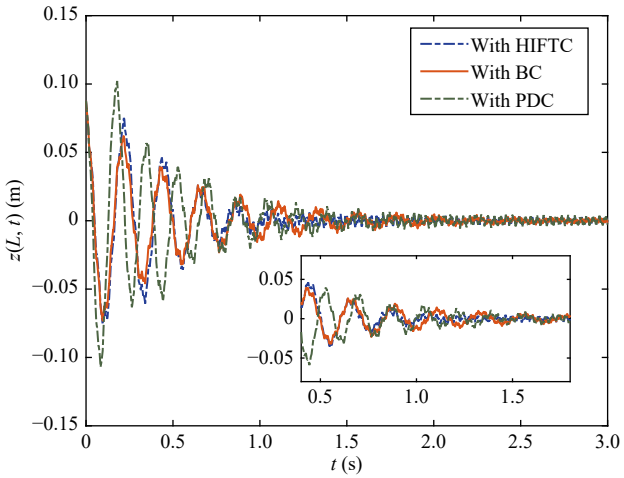

Fig. 4. End-point offset $z(L,t)$.

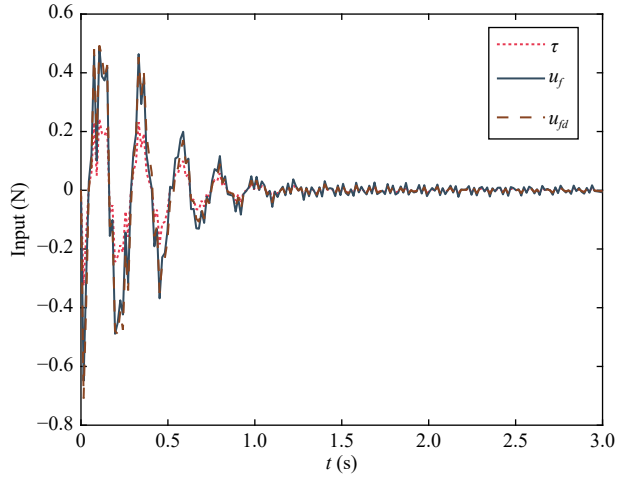

Fig. 5. Control input under the HIFTC controller.

maintained. Therefore, it can be concluded that the HIFTC can better stabilize a flexible manipulator system with unknown hysteresis and intermittent actuator faults.

V. Experiment

To further verify the effectiveness of the proposed control

strategy, physical experiments are performed on the Quanser experimental platform, as shown in Fig. 6. The Quanser experimental platform is the most crucial component of this platform. It consists of a DC motor encased in a robust aluminum frame and a planetary gearbox. Additionally, the motor is equipped with an internal gearbox, enabling it to drive other gears. The basic unit of the Quanser experimental platform is equipped with a potentiometer sensor, which is used to measure the angular position of the load gear. The tip deflection angle is obtained using a strain gauge fixed on the rotary flexible beam. As illustrated in Fig. 6, the system also includes other key components such as a power amplifier, a filter device, a data acquisition board, a host computer, and a digital multimeter. The power amplifier and filter primarily serve to process signals from the aforementioned sensors. The data acquisition board is responsible for A/D conversion and is connected to both the filter and the host. Upon receiving these signals, the host executes the control algorithm and generates the control input signal.

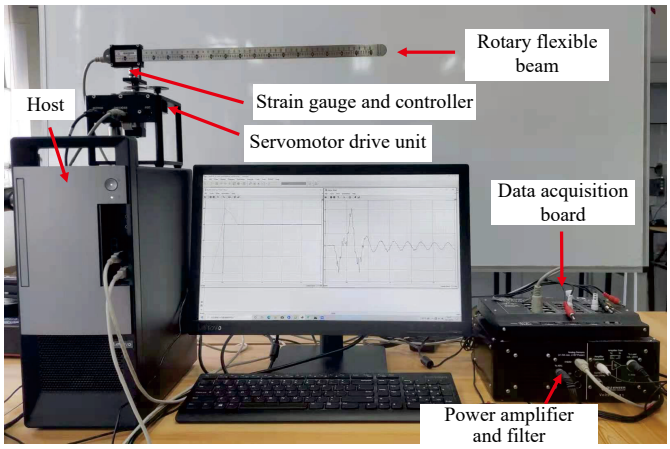

Fig. 6. Rotary flexible link system.

The control strategies are also compared, and the parameters are selected by simulation. The experimental results are shown in Figs. 7−9. Table I summarizes the tracking performance under HIFTC, PDC, and BC. In terms of angular tracking performance, the tracking error of the system utilizing the control strategy proposed in this study decreased by 87.10% compared to BC, and by 97.84% compared to PDC. Moreover, under HIFTC, the system's adaptation time is significantly reduced by 72.50% and 136.08% compared to BC and PDC, respectively, demonstrating a considerable enhancement in performance. As shown in Fig. 7, the HIFTC can track target angles θ_d in the face of system input hysteresis and intermittent actuator faults, whereas BC and PDC cannot meet the preset angle-tracking performance requirements. From Fig. 8, it can be observed that based on HIFTC, the angle error $\theta_e(t)$ converges well to zero, while other strategies exhibit certain steady-state errors. In addition, the deformation of the endpoint can converge uniformly under HIFTC, and the range of convergence depends on the selection of parameters, as shown in Fig. 9. In summary, the simulation and experimental results demonstrate that the proposed controller can better stabilize a flexible manipulator system with

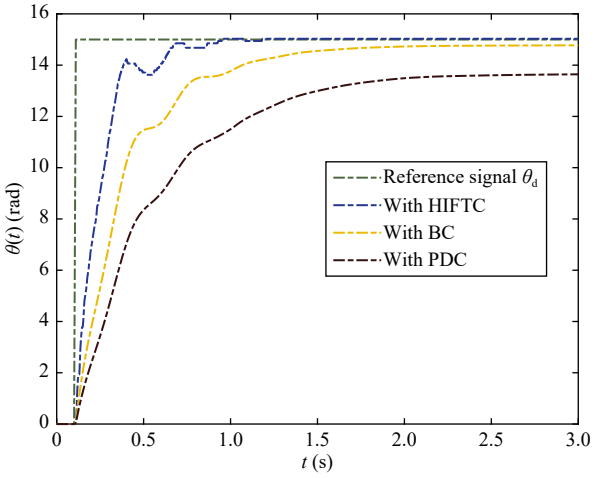

Fig. 7. Angle tracking $\theta(t)$.

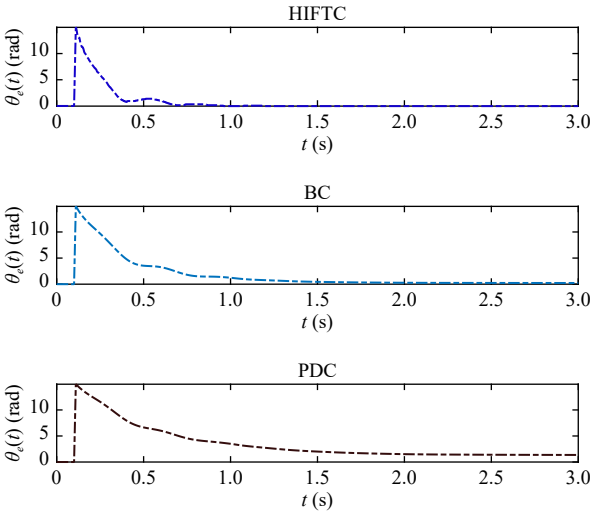

Fig. 8. Angle tracking error $\theta_e(t)$.

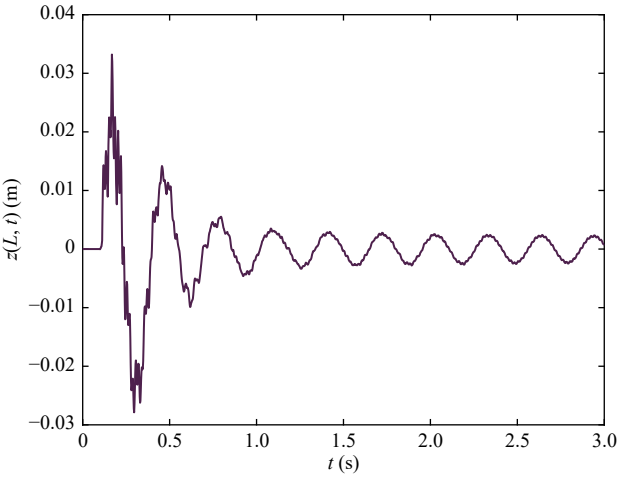

Fig. 9. End-point offset $z(L,t)$.

intermittent actuator faults and unknown hysteresis.

VI. Conclusion

In this study, a new adaptive NN-based FTC strategy is pro-

TABLE I
COMPARISON OF SYSTEM PERFORMANCE BASED ON DIFFERENT APPROACHES IN EXPERIMENT

Tracking performance			
Methods	Overshoot (%)	Accommodation time (s)	Steady-state error (rad)
HIFTC	0.0063	0.6261	0.0293
BC	0	1.0800	0.2272
PDC	0	1.4781	1.3582

posed to stabilize a single-link flexible manipulator system affected by an unknown Bouc-Wen type of hysteresis and intermittent actuator faults. Using the hysteresis inverse dynamics model, the input hysteresis effect of the system was effectively counteracted. Furthermore, an unknown upper-bound adaptive compensation strategy was proposed to offset the side effects caused by the compensation error and produce an uncontrollable additive actuation fault. The designed control ensured the consistency and boundedness of the controlled system, and the control performance was further evaluated through simulation and experimental analysis.

APPENDIX A
PROOF OF LEMMA 4

Based on the Young's inequality (see Lemma 1 in [42]), the inequality holds

$$\begin{aligned}|V_3(t)| &\le \beta_2\rho L\int_0^L|\theta_e\dot{q}|dy+\beta_2\rho\int_0^L|z\dot{q}|dy\\ &\le \frac{\beta_2\rho(1+L)}{2\pi_1}\int_0^L\dot{q}^2dy+\frac{\beta_2\rho L^2\pi_1}{2}\theta_e^2\\ &\quad+\frac{\beta_2\rho L^2\pi_1}{2}\int_0^L z'^2dy\le\lambda_1(V_1(t)+V_2(t))\end{aligned}\tag{45}$$

where $\pi_1\in\mathbb{R}^+$, $\lambda_1=\max\{\frac{\beta_2(1+L)}{\pi_1\alpha},\frac{\beta_2\rho L^2\pi_1}{k_\theta\alpha},\frac{\beta_2\rho L^2\pi_1}{T\alpha}\}$.

Let λ_1 satisfy $0<\lambda_1<1$, we obtain

$$0\le\lambda_2[V_1(t)+V_2(t)]\le V(t)\le\lambda_3[V_1(t)+V_2(t)]\tag{46}$$

where $\lambda_2=1-\lambda_1$ and $\lambda_3=1+\lambda_1$ are positive constants. ■

APPENDIX B
PROOF OF LEMMA 5

By differentiating (28) and substituting (1)–(3), we obtain

$$\dot{V}_1(t)=-\alpha\dot{\theta}(t)[Tz_L+EIz_0'']-c\alpha\int_0^L[\dot{q}(y,t)]^2dy.\tag{47}$$

Applying Lemma 1, (4), (20) and (21) to $\dot{V}_2(t)$ generates the following:

$$\begin{aligned}\dot{V}_2(t)&=u_a(t)[\tau(t)+EIz_0''+Tz_L+I\beta_2\dot{\theta}(t)]+k_\theta\theta_e\dot{\theta}+\dot{V}_k(t)\\ &=u_a(t)[\sigma(t)u_{fd}(t)+\sigma(t)\tilde{\mu}^T\aleph_d+\sigma(t)d(t)+Tz_L\\ &\quad+u_{f,h}(t)+EIz_0''+I\beta_2\dot{\theta}(t)]+k_\theta\theta_e\dot{\theta}+\dot{V}_k(t)\\ &=u_a(t)[\sigma(t)u_a(t)z_1(t)\hat{\varrho}(t)+\sigma(t)\tilde{\mu}^T\aleph_d+\sigma(t)d(t)\\ &\quad+Tz_L+u_{f,h}(t)+EIz_0''+I\beta_2\dot{\theta}(t)]+\dot{V}_k(t)+k_\theta\theta_e\dot{\theta}\\ &=-\sigma(t)(\varrho-\tilde{\varrho})z_1(t)u_a^2(t)+k_\theta\theta_e\dot{\theta}+Tu_a(t)z_L\\ &\quad+EIu_a(t)z_0''+I\beta_2u_a(t)\dot{\theta}(t)+u_a(t)\sigma(t)\tilde{\mu}^T\aleph_d\\ &\quad+u_a(t)u_{f,h}(t)+\sigma(t)u_a(t)d(t)+\dot{V}_k(t)\end{aligned}\tag{48}$$

where $\dot{V}_k$ is defined as

$$\dot{V}_k(t)=-\tilde{\mu}^T\Gamma_\mu^{-1}\dot{\hat{\mu}}-\frac{\sigma}{\gamma_\varrho}\tilde{\varrho}\dot{\hat{\varrho}}-\frac{1}{\gamma_h}\tilde{\hbar}\dot{\hat{\hbar}}-Tr\{\tilde{p}^T\Gamma_p^{-1}\dot{\hat{p}}\}.\tag{49}$$

Let $Y(t)=\sigma(t)\tilde{\mu}^T\aleph_d+\sigma(t)d(t)+u_{f,h}(t)$, according (15) and (16), we derive

$$\begin{aligned}Y(t)&=\tilde{\mu}^T[p^TH(W)+\varepsilon(W)]+\sigma(t)d(t)+u_{f,h}(t)\\ &=\tilde{\mu}^T\hat{p}^TH(W)-\hat{\mu}^T\tilde{p}^TH(W)+\mu^T\tilde{p}^TH(W)\\ &\quad+\tilde{\mu}^T\varepsilon(W)+\sigma(t)d(t)+u_{f,h}(t)\\ &\le\tilde{\mu}^T\hat{p}^TH(W)-\hat{\mu}^T\tilde{p}^TH(W)+\hbar.\end{aligned}\tag{50}$$

Thus, we get

$$\begin{aligned}\dot{V}_2(t)\le&-\underline{\sigma}(\varrho-\tilde{\varrho})z_1(t)u_a^2(t)+u_a(t)[\tilde{\mu}^T\hat{p}^TH(W)\\ &-\hat{\mu}^T\tilde{p}^TH(W)+\hbar]+EIu_a(t)z_0''+k_\theta\theta_e\dot{\theta}\\ &+Tu_a(t)z_L+I\beta_2u_a(t)\dot{\theta}(t)+\dot{V}_k(t).\end{aligned}\tag{51}$$

According to Young's inequality (see Lemma 1 in [42]), (51) can be expressed as

$$\begin{aligned}\dot{V}_2(t)\le&-ku_a^2(t)+\underline{\sigma}\tilde{\varrho}z_1(t)u_a^2(t)+u_a(t)[\tilde{\mu}^T\hat{p}^TH(W)\\ &-\hat{\mu}^T\tilde{p}^TH(W)]-\frac{k_1}{4\delta}\dot{\theta}^2(t)+EIu_a(t)z_0''\\ &-k_\theta\beta_2\theta_e^2(t)+\delta_0+\dot{V}_k(t)\end{aligned}\tag{52}$$

where $\delta_0=\frac{\delta}{4}[I\beta_2+T+k_\theta+1]+\bar{r}$.

Using the adaptive laws (22)–(25), Lemma 3, and Young's inequality (see Lemma 1 in [42]), we then obtain

$$\begin{aligned}\dot{V}_2(t)\le&-ku_a^2(t)-\frac{k_1}{4\delta}\dot{\theta}^2(t)+EIu_a(t)z_0''-\frac{k_\theta\beta_2}{\alpha}\theta_e^2(t)\\ &+\delta_0+\frac{1}{2}(\hbar^2-\tilde{\hbar}^2)-\frac{1}{2}\|\tilde{p}\|_F^2+\frac{1}{2}\|p^*\|_F^2\\ &+\frac{\sigma}{2}\varrho^2-\frac{\sigma}{2}\tilde{\varrho}^2-\frac{\tilde{\mu}^T\Gamma_\mu^{-1}\tilde{\mu}}{2\lambda_{\max}(\Gamma_\mu^{-1})}+\frac{1}{2}\mu^2.\end{aligned}\tag{53}$$

Invoking the PDE model (1)–(4) and Young's inequality (see Lemma 1 in [42]), $\dot{V}_3(t)$ is calculated as

$$\begin{aligned}\dot{V}_3(t)=&-\beta_2EI\int_0^L[z''(y,t)]^2dy-T\beta_2\int_0^L[z'(y,t)]^2dy\\ &-\beta_2c\int_0^Lq_e(y,t)\dot{q}(y,t)dy-\beta_2T\theta_e(t)z_L\\ &-EI\beta_2\theta_e(t)z_0''+\beta_2\rho\int_0^L[\dot{q}(y,t)]^2dy.\end{aligned}\tag{54}$$

By substituting (47), (53), and (54) into $\dot{V}(t)$, we derive

$$\begin{aligned}\dot{V}(t)\le&-\alpha\dot{\theta}(t)[Tz_L+EIz_0'']-c\alpha\int_0^L[\dot{q}(y,t)]^2dy\\ &-ku_a^2(t)-\frac{k_1}{4\delta}\dot{\theta}^2(t)+EIu_a(t)z_0''-\frac{k_\theta\beta_2}{\alpha}\theta_e^2(t)\end{aligned}$$

$$+\delta_0+\frac{1}{2}(\hbar^2-\tilde{\hbar}^2)-\frac{1}{2}\|\tilde{p}\|_F^2+\frac{1}{2}\|p^*\|_F^2$$
$$+\frac{\underline{\sigma}}{2}\varrho^2-\frac{\underline{\sigma}}{2}\tilde{\varrho}^2-\frac{\tilde{\mu}^T\Gamma_\mu^{-1}\tilde{\mu}}{2\lambda_{\max}(\Gamma_\mu^{-1})}+\frac{1}{2}\mu^2$$
$$-\beta_2 EI\int_0^L[z''(y,t)]^2dy-T\beta_2\int_0^L[z'(y,t)]^2dy$$
$$-\beta_2 c\int_0^L q_e(y,t)\dot{q}(y,t)dy-\beta_2 T\theta_e(t)z_L$$
$$-EI\beta_2\theta_e(t)z_0''+\beta_2\rho\int_0^L[\dot{q}(y,t)]^2dy. \tag{55}$$

Invoking $u_a(t)=\alpha\dot{\theta}(t)+\beta_2\theta_e(t)\Rightarrow\dot{\theta}(t)=\frac{u_a(t)-\beta_2\theta_e(t)}{\alpha(t)}$, we obtain

$$\dot{V}(t)\le-\alpha[\frac{u_a(t)-\beta_2\theta_e(t)}{\alpha(t)}][Tz_L+EIz_0'']-EI\beta_2\theta_e(t)z_0''$$
$$-ku_a^2(t)-\frac{k_1}{4\delta}[\frac{u_a(t)-\beta_2\theta_e(t)}{\alpha(t)}]^2+EIu_a(t)z_0''$$
$$-\frac{k_\theta\beta_2}{\alpha}\theta_e^2(t)+\delta_0+\frac{1}{2}(\hbar^2-\tilde{\hbar}^2)-\frac{1}{2}\|\tilde{p}\|_F^2+\frac{1}{2}\|p^*\|_F^2$$
$$+\frac{\underline{\sigma}}{2}\varrho^2-\frac{\underline{\sigma}}{2}\tilde{\varrho}^2-\frac{\tilde{\mu}^T\Gamma_\mu^{-1}\tilde{\mu}}{2\lambda_{\max}(\Gamma_\mu^{-1})}+\frac{1}{2}\mu^2-\beta_2 T\theta_e(t)z_L$$
$$-\beta_2 EI\int_0^L[z''(y,t)]^2dy-T\beta_2\int_0^L[z'(y,t)]^2dy$$
$$-\beta_2 c\int_0^L z(y,t)\dot{q}(y,t)dy-\beta_2 c\int_0^L y\theta_e(t)\dot{q}(y,t)dy$$
$$-c\alpha\int_0^L[\dot{q}(y,t)]^2dy+\beta_2\rho\int_0^L[\dot{q}(y,t)]^2dy. \tag{56}$$

Furthermore, we get

$$\dot{V}(t)\le-(c\alpha-\rho\beta_2-\frac{c\beta_2(1+L)}{2})\int_0^L\dot{q}^2(y,t)dy-(T\beta_2$$
$$-\frac{\beta_2 cL^2}{2}-\frac{TL}{2\pi_3})\int_0^L[z'(y,t)]^2dy-(\varpi_0-\frac{k_1\beta_2}{2\delta\pi_2\alpha^2}$$
$$-\frac{T\pi_3}{2})[u_a(t)]^2-\beta_2 EI\int_0^L[z''(y,t)]^2dy$$
$$-(\frac{k_1\beta_2^2}{4\delta\alpha^2}+\frac{k_\theta\beta_2}{\alpha}-\frac{\beta_2 cL^2}{2}-\frac{k_1\beta_2\pi_2}{2\delta\alpha^2})\theta_e^2(t)$$
$$+\iota-\frac{\tilde{\mu}^T\Gamma_\mu^{-1}\tilde{\mu}}{2\lambda_{\max}(\Gamma_\mu^{-1})}-\frac{1}{2}\tilde{\hbar}^2-\frac{1}{2}\|\tilde{p}\|_F^2-\frac{\underline{\sigma}}{2}\tilde{\varrho}^2 \tag{57}$$

where $\varpi_0=k+\frac{k_1}{4\delta\alpha^2}$, $\pi_2,\pi_3\in\mathbb{R}^+$, and $\iota=\frac{1}{2}\hbar^2+\frac{1}{2}\|p^*\|_F^2+\frac{\underline{\sigma}}{2}\varrho^2+\frac{1}{2}\mu^2+\delta_0$.

The constraint conditions that allow (57) to hold are as follows:

$$\varpi_1=c\alpha-\rho\beta_2-\frac{c\beta_2(1+L)}{2}>0 \tag{58}$$

$$\varpi_2=T\beta_2-\frac{\beta_2 cL^2}{2}-\frac{TL}{2\pi_3}>0 \tag{59}$$

$$\varpi_3=\varpi_0-\frac{k_1\beta_2}{2\delta\pi_2\alpha^2}-\frac{T\pi_3}{2}>0 \tag{60}$$

$$\varpi_4=\frac{k_\theta\beta_2}{\alpha^2}+\frac{k_1\beta_2^2}{4\delta\alpha^2}-\frac{\beta_2 cL^2}{2}-\frac{k_1\beta_2\pi_2}{2\delta\alpha^2}>0 \tag{61}$$

$$\iota=\frac{1}{2}\hbar^2+\frac{1}{2}\|p^*\|_F^2+\frac{\underline{\sigma}}{2}\varrho^2+\frac{1}{2}\mu^2+\delta_0<+\infty. \tag{62}$$

In addition, by employing Lemma 4 and (58)–(62), we obtain

$$\dot{V}(t)\le-\lambda V(t)+\iota \tag{63}$$

where $\lambda\le\frac{1}{\lambda_3}\min(\frac{2\varpi_1}{\rho\alpha},\frac{2\varpi_2}{T\alpha},\frac{2\varpi_3}{I\alpha},\frac{2\varpi_4}{k_\theta\alpha},\frac{1}{\lambda_{\max}(\Gamma_\mu^{-1})},\frac{1}{\lambda_{\max}(\Gamma_p^{-1})},\gamma_\varrho,\gamma_h)$. ■

REFERENCES

[1] H. Huang, W. He, Q. Fu, X. He, and C. Sun, "A bio-inspired flapping-wing robot with cambered wings and its application in autonomous airdrop," *IEEE/CAA J. Autom. Sinica*, vol. 9, no. 12, pp. 2138–2150, 2022.

[2] Z. Zhao and Z. Liu, "Finite-time convergence disturbance rejection control for a flexible Timoshenko manipulator," *IEEE/CAA J. Autom. Sinica*, vol. 8, no. 1, pp. 157–168, 2021.

[3] Z.-H. Luo, B.-Z. Guo, and Ö. Morgül, *Stability and Stabilization of Infinite Dimensional Systems With Applications*, London, UK: Springer Science & Business Media, 2012.

[4] X. Zhao, S. Zhang, Z. Liu, J. Wang, and H. Gao, "Adaptive event-triggered boundary control for a flexible manipulator with input quantization," *IEEE/ASME Trans. Mechatronics*, vol. 27, no. 5, pp. 3706–3716, 2022.

[5] T. Jiang, J. Liu, and W. He, "Boundary control for a flexible manipulator with a robust state observer," *J. Vibration and Control*, vol. 24, no. 2, pp. 260–271, 2018.

[6] J. Wang, H. Zhang, K. Ma, Z. Liu, and C. L. P. Chen, "Neural adaptive self-triggered control for uncertain nonlinear systems with input hysteresis," *IEEE Trans. Neural Networks and Learning Syst.*, vol. 33, no. 11, pp. 6206–6214, 2022.

[7] X. Chen and T. Ozaki, "Adaptive control for plants in the presence of actuator and sensor uncertain hysteresis," *IEEE Trans. Autom. Control*, vol. 56, no. 1, pp. 171–177, 2010.

[8] M. Chen and S. S. Ge, "Adaptive neural output feedback control of uncertain nonlinear systems with unknown hysteresis using disturbance observer," *IEEE Trans. Industrial Electronics*, vol. 62, no. 12, pp. 7706–7716, 2015.

[9] Z. Li, Z. Li, H. Xu, X. Zhang, and C.-Y. Su, "Development of a butterfly fractional-order backlash-like hysteresis model for dielectric elastomer actuators," *IEEE Trans. Industrial Electronics*, vol. 70, no. 2, pp. 1794–1801, 2023.

[10] Y. Cheng, B. Niu, X. Zhao, G. Zong, and A. M. Ahmad, "Event-triggered adaptive decentralised control of interconnected nonlinear systems with Bouc-Wen hysteresis input," *Int. J. Syst. Science*, vol. 54, no. 6, pp. 1275–1288, 2023.

[11] X. Liu, Y. Wu, N. Wu, H. Yan, and Y. Wang, "Finite-time-prescribed performance-based adaptive command filtering control for mimo nonlinear systems with unknown hysteresis," *Nonlinear Dynamics*, vol. 111, no. 8, pp. 7357–7375, 2023.

[12] Z. Zhao, Z. Liu, W. He, K.-S. Hong, and H.-X. Li, "Boundary adaptive fault-tolerant control for a flexible Timoshenko arm with backlash-like hysteresis," *Automatica*, vol. 130, p. 109690, 2021.

[13] W. He and T. Meng, "Adaptive control of a flexible string system with input hysteresis," *IEEE Trans. Control Syst. Techn.*, vol. 26, no. 2, pp. 693–700, 2018.

[14] J. Zhang, X. Xiang, W. Li, and Q. Zhang, "Adaptive saturated path following control of underactuated AUV with unmodeled dynamics and unknown actuator hysteresis," *IEEE Trans. Syst., Man, and Cybern.: Syst.*, vol. 53, no. 10, pp. 6018–6030, 2023.

[15] G. Tao and P. V. Kokotovic, "Adaptive control of plants with unknown

hystereses," *IEEE Trans. Autom. Control*, vol. 40, no. 2, pp. 200–212, 1995.

[16] Y. Wang, X. Zhang, Z. Li, X. Chen, and C.-Y. Su, "Adaptive implicit inverse control for a class of butterfly-like hysteretic nonlinear systems and its application to dielectric elastomer actuators," *IEEE Trans. Industrial Electronics*, vol. 70, no. 1, pp. 731–740, 2023.

[17] J. Zhou, C. Wen, and T. Li, "Adaptive output feedback control of uncertain nonlinear systems with hysteresis nonlinearity," *IEEE Trans. Autom. Control*, vol. 57, no. 10, pp. 2627–2633, 2012.

[18] K. Lu, Z. Liu, C. Chen, and Y. Zhang, "Adaptive inverse compensation for unknown input and output hysteresis using output feedback neural control," *IEEE Trans. Syst., Man, and Cybern.: Syst.*, vol. 52, no. 5, pp. 3224–3236, 2021.

[19] Z. Liu, K. Lu, G. Lai, C. L. P. Chen, and Y. Zhang, "Indirect fuzzy control of nonlinear systems with unknown input and state hysteresis using an alternative adaptive inverse," *IEEE Trans. Fuzzy Syst.*, vol. 29, no. 3, pp. 500–514, 2021.

[20] C. Wang, L. Guo, C. Wen, Q. Hu, and J. Qiao, "Event-triggered adaptive attitude tracking control for spacecraft with unknown actuator faults," *IEEE Trans. Industrial Electronics*, vol. 67, no. 3, pp. 2241–2250, 2020.

[21] Z. Liu, Z. Han, and W. He, "Adaptive fault-tolerant boundary control of an autonomous aerial refueling hose system with prescribed constraints," *IEEE Trans. Autom. Science and Engineering*, vol. 19, no. 4, pp. 2678–2688, 2022.

[22] Z. Liu, J. Liu, and W. He, "Robust adaptive fault tolerant control for a linear cascaded ODE-beam system," *Automatica*, vol. 98, pp. 42–50, 2018.

[23] S. Zhang, Y. Wu, X. He, and Z. Liu, "Cooperative fault-tolerant control for a mobile dual flexible manipulator with output constraints," *IEEE Trans. Autom. Science and Engineering*, vol. 19, no. 4, pp. 2689–2698, 2022.

[24] L. Li, F. Cao, and J. Liu, "Adaptive vibration control for constrained moving vehicle-mounted nonlinear 3D rigid-flexible manipulator system subject to actuator failures," *J. Vibration and Control*, vol. 29, no. 17–18, pp. 4155–4171, 2023.

[25] W. Wang and C. Wen, "Adaptive compensation for infinite number of actuator failures or faults," *Automatica*, vol. 47, no. 10, pp. 2197–2210, 2011.

[26] Y. Ma, X. He, S. Zhang, Y. Sun, and Q. Fu, "Adaptive compensation for infinite number of actuator faults and time-varying delay of a flexible manipulator system," *IEEE Trans. Industrial Electronics*, vol. 69, no. 12, pp. 13141–13150, 2022.

[27] Y. Ren, M. Chen, and J. Liu, "Bilateral coordinate boundary adaptive control for a helicopter lifting system with backlash-like hysteresis," *Science China Information Sciences*, vol. 63, no. 1, pp. 1–3, 2020.

[28] K. E. Majdoub, F. Giri, and F.-Z. Chaoui, "Adaptive backstepping control design for semi-active suspension of half-vehicle with magnetorheological damper," *IEEE/CAA J. Autom. Sinica*, vol. 8, no. 3, pp. 582–596, 2021.

[29] M. Rakotondrabe, "Bouc-Wen modeling and inverse multiplicative structure to compensate hysteresis nonlinearity in piezoelectric actuators," *IEEE Trans. Autom. Science and Engineering*, vol. 8, no. 2, pp. 428–431, 2011.

[30] Z. Zhao, Y. Liu, T. Zou, K.-S. Hong, and H.-X. Li, "Robust adaptive fault-tolerant control for a riser-vessel system with input hysteresis and time-varying output constraints," *IEEE Trans. Cybern.*, vol. 53, no. 6, pp. 3939–3950, 2022.

[31] X. Zhang, Y. Wang, C. Wang, C.-Y. Su, Z. Li, and X. Chen, "Adaptive estimated inverse output-feedback quantized control for piezoelectric positioning stage," *IEEE Trans. Cybern.*, vol. 49, no. 6, pp. 2106–2118, 2019.

[32] W. Wu, Y. Li, and S. Tong, "Neural network output-feedback consensus fault-tolerant control for nonlinear multiagent systems with intermittent actuator faults," *IEEE Trans. Neural Networks and Learning Syst.*, vol. 34, no. 8, pp. 1–13, 2021.

[33] S. Xu and B. He, "Robust adaptive fuzzy fault tolerant control of robot manipulators with unknown parameters," *IEEE Trans. Fuzzy Syst.*, vol. 31, no. 9, pp. 3081–3092, 2023.

[34] H. Yang and J. Liu, "An adaptive rbf neural network control method for a class of nonlinear systems," *IEEE/CAA J. Autom. Sinica*, vol. 5, no. 2, pp. 457–462, 2018.

[35] W. Wu, Y. Li, and S. Tong, "Neural network output-feedback consensus fault-tolerant control for nonlinear multiagent systems with intermittent actuator faults," *IEEE Trans. Neural Networks and Learning Systems*, vol. 34, no. 8, pp. 4728–4740, 2021.

[36] W. Wang, C. Wen, J. Huang, and J. Zhou, "Adaptive consensus of uncertain nonlinear systems with event triggered communication and intermittent actuator faults," *Automatica*, vol. 111, p. 108667, 2020.

[37] Y.-X. Li and G.-H. Yang, "Adaptive asymptotic tracking control of uncertain nonlinear systems with input quantization and actuator faults," *Automatica*, vol. 72, pp. 177–185, 2016.

[38] Z. Zhao, Z. Tan, Z. Liu, M. O. Efe, and C. K. Ahn, "Adaptive inverse compensation fault-tolerant control for a flexible manipulator with unknown dead-zone and actuator faults," *IEEE Trans. Industrial Electronics*, vol. 70, no. 12, pp. 12698–12707, 2023.

[39] F. Cao and J. Liu, "Adaptive actuator fault compensation control for a rigid-flexible manipulator with ODEs-PDEs model," *Int. J. Syst. Science*, vol. 49, no. 8, pp. 1748–1759, 2018.

[40] M. Kharrat, "Neural networks-based adaptive fault-tolerant control for stochastic nonlinear systems with unknown backlash-like hysteresis and actuator faults," *J. Applied Mathematics and Computing*, vol. 70, no. 3, pp. 1–24, 2024.

[41] K. Xu, H. Wang, and P. X. Liu, "Command filter-based adaptive fixed-time fault-tolerant control for stochastic nonlinear systems with actuator hysteresis," *Asian J. Control*, vol. 26, no. 3, pp. 1602–1613, 2023.

[42] Y. Ma, X. He, M. Chen, and W. He, "Predictor-based control for a flexible satellite subject to output time delay," *IEEE Trans. Control Syst. Technology*, vol. 30, no. 4, pp. 1420–1432, 2022.

[43] X. He, S. Zhang, Y. Ouyang, and Q. Fu, "Vibration control for a flexible single-link manipulator and its application," *IET Control Theory & Applications*, vol. 14, no. 7, pp. 930–938, 2020.

Shouyan Chen received the B.Eng. degree in process control and the Ph.D. degree in mechanical design from the South China University of Technology, in 2008 and 2017, respectively. He is currently an Associate Professor at the School of Mechanical and Electrical Engineering, Guangzhou University. His research interests include robotics, human-robot interaction, and intelligent control.

Weitian He received the M.S. degree in traffic transportation from Guangzhou University in 2023. He is currently a Ph.D. candidate in control theory and control engineering at the School of Control Science and Engineering and the Center for Intelligent Medical Engineering, Shandong University. His research interests include deterministic learning theory, adaptive learning control, intelligent control, and robotics.

Zhijia Zhao (Member, IEEE) received the B.Eng. degree in automatic control in systems engineering from North China University of Water Resources and Electric Power in 2010, and the M.Eng. and Ph.D. degrees in automatic control from South China University of Technology in 2013 and 2017, respectively. He is currently a Professor at the School of Mechanical and Electrical Engineering, Guangzhou University. His research interests include adaptive and learning control, flexible mechanical systems, and robotics.

Yun Feng received the Ph.D. degree from the Department of Systems Engineering and Engineering Management, City University of Hong Kong, China in 2020. He is currently an Associate Professor in the College of Electrical and Information Engineering, Hunan University, and also with the National Engineering Laboratory for Robot Visua Perception and Control Technology, Hunan University. His research interests include distributed parameter systems, fault diagnosis, and soft robotics. He was selected for the Young Elite Scientists Sponsorship Program by the China Association for Science and Technology in 2023.

Zhijie Liu (Member, IEEE) received the B.Sc. degree in electrical engineering and automation from the China University of Mining and Technology Beijing in 2014 and the Ph.D. degree in control theory and control engineering from Beihang University in 2019, both in automatic control. In 2017, he was a Research Assistant with the Department of Electrical Engineering, University of Notre Dame, USA, for 12 months. He is currently a Professor with the School of Intelligence Science and Technology, University of Science and Technology Beijing. His research interests include adaptive control, modeling and vibration control for flexible structures, and distributed parameter systems.

Keum-Shik Hong (Fellow, IEEE) received the B.S. degree in mechanical design from Seoul National University, South Korea in 1979, the M.S. degree in mechanical engineering from Columbia University, USA in 1987, and the M.E. degree in applied mathematics and the Ph.D. degrees in mechanical engineering from the University of Illinois at Urbana-Champaign, USA in 1991 and 1997, respectively. He joined the School of Mechanical Engineering, Pusan National University, South Korea in 1993. His research interests include brain-computer interface, nonlinear systems theory, adaptive control, and distributed parameter systems.

Dr. Hong served as an Associate Editor of *Automatica* (2000–2006), as the Editor-in-Chief of the *Journal of Mechanical Science and Technology* (2008–2011), and serving as the Editor-in-Chief for the *International Journal of Control, Automation, and Systems*. He was the past President of the Institute of Control, Robotics and Systems (ICROS), South Korea, and the President of the Asian Control Association. He is a Fellow of the Korean Academy of Science and Technology, an ICROS Fellow, and a Member of the National Academy of Engineering of Korea. He has received many awards, including the Best Paper Award from the KFSTS of Korea in 1999 and the Presidential Award of Korea in 2007.